RESEARCH ARTICLE | JUNE 08 2023

Nonadiabatic dynamics near metal surface with periodic drivings: A Floquet surface hopping algorithm

Yu Wang ; Wenjie Dou

J. Chem. Phys. 158, 224109 (2023)
https://doi.org/10.1063/5.0148418

The Journal of Chemical Physics ARTICLE scitation.org/journal/jcp

Nonadiabatic dynamics near metal surface with periodic drivings: A Floquet surface hopping algorithm

Cite as: J. Chem. Phys. 158, 224109 (2023); doi: 10.1063/5.0148418
Submitted: 1 March 2023 • Accepted: 23 May 2023 •
Published Online: 8 June 2023

Yu Wang[1,2,a] and Wenjie Dou[1,2,3,b]

AFFILIATIONS

[1] Department of Chemistry, School of Science, Westlake University, Hangzhou 310024, Zhejiang, China
[2] Institute of Natural Sciences, Westlake Institute for Advanced Study, Hangzhou 310024, Zhejiang, China
[3] Department of Physics, School of Science, Westlake University, Hangzhou 310024, Zhejiang, China

[a] Author to whom correspondence should be addressed: wangyu19@westlake.edu.cn
[b] Electronic mail: douwenjie@westlake.edu.cn

ABSTRACT

We develop a Floquet surface hopping approach to deal with nonadiabatic dynamics of molecules near metal surfaces subjected to time-periodic drivings from strong light–matter interactions. The method is based on a Floquet classical master equation (FCME) derived from a Floquet quantum master equation (FQME), followed by a Wigner transformation to treat nuclear motion classically. We then propose different trajectory surface hopping algorithms to solve the FCME. We find that a Floquet averaged surface hopping with electron density (FaSH-density) algorithm works the best as benchmarked with the FQME, capturing both the fast oscillations due to the driving and the correct steady-state observables. This method will be very useful to study strong light–matter interactions with a manifold of electronic states.

I. INTRODUCTION

Floquet engineering is a powerful tool to control the dynamics of quantum systems using time-periodic external fields (e.g., electromagnetic fields), which accounts for various phenomena.[1] In practice, a surface plasmon or a Fabry–Pérot cavity can create a resonant electromagnetic (EM) field and realize Floquet engineering through strong light–matter interactions. For instance, strong light–matter coupling is achieved by placing materials in a resonance EM field and shows great promise to control the properties of matter without structural modifications.[2,3] In addition, n-type or p-type organic semiconductors deposited on top of a metal surface, which acts as an open electromagnetic cavity, have been observed a noteworthy conductivity enhancement.[4,5] Moreover, strong light–matter coupling can largely extend the spatial range of energy transport in organic materials.[6–8] Furthermore, numerous photophysical and photochemical properties, such as electronic relaxation pathways,[9–11] quantum yields,[12–15] and chemical reactivities,[16–19] can also be manipulated in the strong coupling regime. The microscopic mechanisms leading to these modifications through strong light–matter interactions, however, remain largely unexplained. In a recent article, the authors showed the connection between Floquet theory and quantum electrodynamics in an optical cavity.[20]

On the one hand, without Floquet driving, when nuclei interact non-adiabatically with a manifold of electronic states (e.g., an adsorbate at a metal surface), there is a drastic breakdown of the Born–Oppenheimer approximation. There are several numerically exact solutions for such non-adiabatic processes when only a few degrees of freedom (DoFs) are considered, including multiconfiguration time-dependent Hartree (MCTDH),[21] quantum Monte Carlo (QMC),[22] numerical renormalization group (NRG),[23–25] and hierarchical quantum master equation (HQME).[26,27] That being said, these methods are difficult to apply to large, realistic systems. Many attempts have been made to develop approximate methods to deal with realistic systems involving nonadiabatic dynamics in open quantum systems.[28–31] On the other hand, when considering nonadiabatic dynamics under Floquet driving, there exists Floquet surface hopping[32–34] as well as coupled-trajectory mixed quantum–classical[35] methods to study dynamics for a closed system. For open quantum systems, there are far less approaches

available with only a few exceptions, such as the Floquet scattering matrix,[36–38] Floquet–Green's functions,[39–42] and Floquet master equations.[43–45] Again, these methods are only applicable to small systems. Accurate methods are needed to study large and realistic systems.

In this article, we attempt to offer accurate and efficient tools to study nonadiabatic dynamics in open quantum systems with Floquet engineering. We first derive a Floquet quantum master equation (FQME) to accurately uncover the non-adiabatic processes of a periodically driven impurity level near a metal surface. The FQME is only useful for incorporating only one or two phonon modes and/or one or two electronic levels. For many nuclear DoFs and arbitrary electron-nuclear couplings, we will employ a Floquet classical master equation (FCME), which is achieved by taking the Wigner transformation of FQME, similar to the steps in Ref. 46 for a non-Floquet scenario. We then propose three Floquet surface hopping algorithms to solve the FCME. We find that an algorithm named time-averaged Floquet surface hopping with density (FaSH-density) is able to reproduce full dynamics as well as steady-state results as benchmarked against FQME.

An outline of this paper is as follows: In Sec. II, we outline how to derive the FQME and FCME and present the Floquet surface hopping (FSH) algorithm. In Sec. III, we present the results of both electronic population and phonon relaxation dynamics under different Floquet drivings employing five different methods (FQME, FSH, FaQME, FaSH, and FaSH-density). We conclude in Sec. IV.

II. THEORY

A. Model Hamiltonian

We consider the Newns–Holstein Hamiltonian with one impurity level coupled to a Fermionic bath as well as subjected to periodic driving. The molecule consists of a single electronic level coupled to a single phonon and a manifold of electrons,

$$\hat{H}(t) = \hat{H}_S(t) + \hat{H}_B + \hat{H}_T, \tag{1}$$

$$\hat{H}_S(t) = (E_d + A\,\sin(\Omega t))d^+d + g(a^+ + a)d^+d + \hbar\omega\left(a^+a + \frac{1}{2}\right), \tag{2}$$

$$\hat{H}_B = \sum_k \varepsilon_k c_k^+ c_k, \tag{3}$$

$$\hat{H}_T = \sum_k V_k(d^+c_k + c_k^+ d). \tag{4}$$

$\hat{H}_S(t)$ is the system Hamiltonian with E_d being the energy level and ω being the frequency of the harmonic oscillator. g represents the electron–phonon (el–ph) coupling strength. A is the driving amplitude, and Ω is the driving frequency. In addition, $\hat{H}_B$ represents the bath Hamiltonian with ε_k being the energy level of the fermion c_k in the bath. $\hat{H}_T$ is the interaction Hamiltonian with V_k being the coupling strength between the impurity level d and the fermion c_k in the bath.

Note that we can generalize our FCME into many DoFs and arbitrary electron–phonon coupling easily. For comparison to FQME, we restrict ourselves to one phonon and linear electron–phonon couplings. For a harmonic oscillator, it will be convenient to replace a^+ and a with the position x and momentum p (i.e., $x = \sqrt{\frac{\hbar}{2M\omega}}(a^+ + a)$ and $p = i\sqrt{\frac{M\hbar\omega}{2}}(a^+ - a)$), where M is the nuclear mass, such that the system Hamiltonian can be written as

$$\hat{H}_S = (E_d + A\,\sin(\Omega t))d^+d + \sqrt{\frac{2M\omega}{\hbar}}gxd^+d + \frac{p^2}{2M} + \frac{1}{2}M\omega^2x^2. \tag{5}$$

To derive a Floquet quantum master equation for treating the dynamics of the periodically driven open quantum system, we first separate the time-independent part from the time-dependent part in $H_S(t)$ such that

$$\hat{H}_S(t) = \hat{H}_{mol} + A\,\sin(\Omega t)d^+d, \tag{6}$$

$$\hat{H}_{mol} = \left(E_d + \sqrt{\frac{2M\omega}{\hbar}}gx\right)d^+d + \frac{p^2}{2M} + \frac{1}{2}M\omega^2x^2. \tag{7}$$

We can further write $\hat{H}_{mol}$ as

$$\hat{H}_{mol} = H_0|0\rangle\langle 0| + H_1|1\rangle\langle 1|, \tag{8}$$

$$\hat{H}_0 = \frac{p^2}{2M} + \frac{1}{2}M\omega^2x^2, \tag{9}$$

$$\hat{H}_1 = \frac{p^2}{2M} + \frac{1}{2}M\omega^2x^2 + \sqrt{\frac{2M\omega}{\hbar}}gx + E_d, \tag{10}$$

where $|0\rangle$ ($|1\rangle$) denotes the unoccupied (occupied) state of the impurity. Below, we eliminate the hats over the Hamiltonians for simplicity.

B. Floquet quantum master equation

We now sketch out the derivation of a Floquet quantum master equation for treating the dynamics of the system. The key quantity of interest is the reduced density matrix of the system. Starting with the quantum Liouville equation in the interaction picture, we find that the total density matrix can be expressed as

$$\frac{d\rho(t)}{dt} = -\frac{i}{\hbar}[H_T(t), \rho(0)] - \frac{1}{\hbar^2}\int_0^t dt'[H_T(t), [H_T(t'), \rho(t')]], \tag{11}$$

where

$$H_T(t) = U^+(t)H_TU(t). \tag{12}$$

Here, the time evolution operator $U(t)$ is

$$\begin{aligned} U(t) &= \hat{T}\exp\left[-\frac{i}{\hbar}\int_0^t dt'(H_B + H_S(t'))\right] \\ &= \hat{T}\exp\left[-\frac{i}{\hbar}\int_0^t dt'(H_B + H_{mol} + A\,\sin(\Omega t')d^+d)\right] \\ &= \exp(-i(H_B + H_{mol})t/\hbar - ig(t)d^+d/\hbar), \end{aligned} \tag{13}$$

where $\hat{T}$ is the time ordering operator and $g(t) = \frac{A}{\hbar\Omega}(1 - \cos(\Omega t))$. Note that we have used the fact that the time-dependent term commutes with the system Hamiltonian. In the most general case,

we need to diagonalize the time-dependent Hamiltonian using the Floquet propagator. See Ref. 47.

In the Born–Markovian approximation, we replace $\rho(t')$ in Eq. (11) by $\rho_B^{eq} \otimes \rho_S(t)$ in the integrand that relies on the assumptions that the bath remains in equilibrium throughout the process and that bath correlation functions decay fast on the system time scale. Note that in the Born–Markovian approximation, it is assumed that the bath correlation function decays much faster than the timescale of electron transfer, which is mainly determined by Γ. Although electron transfer is related to periodic drivings, the Born–Markovian approximation still holds in fast drivings. It should be noted that the driving frequency Ω should satisfy $\hbar\Omega \ll |\varepsilon_{\max} - \varepsilon_{\min}|$, where $\varepsilon_{\max}$ and $\varepsilon_{\min}$ are band edges of the metal surface[45] so that the Markovian approximation is appropriate. This leads to (setting $\tau = t - t'$)

$$\frac{d\rho(t)}{dt} = -\frac{i}{\hbar}[H_T(t), \rho(0)] - \frac{1}{\hbar^2}\int_0^\infty d\tau \big[H_T(t), \big[H_T(t-\tau), \rho_B^{eq} \otimes \rho_S(t)\big]\big]. \quad (14)$$

Next, we assume the initial total density matrix is a direct product of the system density matrix and the equilibrium bath density matrix, i.e., $\rho(0) = \rho_B^{eq} \otimes \rho_S(0)$, and take the trace of Eq. (11) over bath degrees of freedom. We also use $\mathrm{Tr}_B(H_T(t)\rho_B^{eq}) = 0$, which yields[48,49]

$$\frac{d\rho_S(t)}{dt} = -\frac{1}{\hbar^2}\int_0^\infty d\tau Tr_B\big[H_T(t), \big[H_T(t-\tau), \rho_B^{eq} \otimes \rho_S(t)\big]\big]. \quad (15)$$

We then go back to Schrödinger picture, $\rho_S(t) = e^{iH_{mol}t}\rho_s e^{-iH_{mol}t}$. We assume $\rho_s = \rho_0|0\rangle\langle 0| + \rho_1|1\rangle\langle 1|$, which ensures that there will be no coherence between occupied and unoccupied states at later time. The reduced density matrix for state 0 (unoccupied) and state 1 (occupied) evolves as

$$\begin{aligned}\frac{d\rho_0}{dt} = &-i[H_0, \rho_0] - \sum_k \frac{|V_k|^2}{\hbar^2} \\ &\times \int_0^\infty d\tau \Big[e^{i\varepsilon_k\tau/\hbar - i(g(t)-g(t-\tau))/\hbar} f(\varepsilon_k) e^{-iH_1\tau/\hbar} e^{iH_0\tau/\hbar}\rho_0 \\ &- e^{i\varepsilon_k\tau/\hbar - i(g(t)-g(t-\tau))/\hbar}(1-f(\varepsilon_k))\rho_1 e^{-iH_1\tau/\hbar} e^{iH_0\tau/\hbar} \\ &+ e^{-i\varepsilon_k\tau/\hbar + i(g(t)-g(t-\tau))/\hbar} f(\varepsilon_k)\rho_0 e^{-iH_0\tau/\hbar} e^{iH_1\tau/\hbar} \\ &- e^{-i\varepsilon_k\tau/\hbar + i(g(t)-g(t-\tau))/\hbar}(1-f(\varepsilon_k)) e^{-iH_0\tau/\hbar} e^{iH_1\tau/\hbar}\rho_1 \Big], \end{aligned} \quad (16)$$

$$\begin{aligned}\frac{d\rho_1}{dt} = &-i[H_1, \rho_1] - \sum_k \frac{|V_k|^2}{\hbar^2} \\ &\times \int_0^\infty d\tau \Big[e^{-i\varepsilon_k\tau/\hbar + i(g(t)-g(t-\tau))/\hbar}(1-f(\varepsilon_k)) e^{-iH_0\tau/\hbar} e^{iH_1\tau/\hbar}\rho_1 \\ &- e^{-i\varepsilon_k\tau/\hbar + i(g(t)-g(t-\tau))/\hbar} f(\varepsilon_k)\rho_0 e^{-iH_0\tau/\hbar} e^{iH_1\tau/\hbar} \\ &+ e^{i\varepsilon_k\tau/\hbar - i(g(t)-g(t-\tau))/\hbar}(1-f(\varepsilon_k))\rho_1 e^{-iH_1\tau/\hbar} e^{iH_0\tau/\hbar} \\ &- e^{i\varepsilon_k\tau/\hbar - i(g(t)-g(t-\tau))/\hbar} f(\varepsilon_k) e^{-iH_1\tau/\hbar} e^{iH_0\tau/\hbar}\rho_0 \Big]. \end{aligned} \quad (17)$$

Here, f is the Fermi function $(f(x) = 1/(1+e^{\beta x}))$. By employing the Jacobi–Anger expansion, we can express $e^{-ig(t)}$ as

$$e^{-ig(t)} = e^{-\frac{i}{\hbar}\frac{A}{\Omega}} e^{\frac{i}{\hbar}\frac{A}{\Omega}\cos(\Omega t)} = e^{-\frac{i}{\hbar}\frac{A}{\Omega}} \sum_{n=-\infty}^{+\infty} (i)^n J_n(z) e^{in\Omega t}, \quad (18)$$

where n is the integer, $J_n(z)$ is the nth Bessel function of the first kind, and $z = \frac{A}{\hbar\Omega}$. Thus, we can expand the term $e^{-i(g(t)-g(t-\tau))/\hbar}$ appearing in Eqs. (16) and (17) as

$$e^{-i(g(t)-g(t-\tau))/\hbar} = \sum_{n,m} (i)^{n-m} J_n(z) J_m(z) e^{i(n-m)\Omega t} e^{im\Omega\tau}. \quad (19)$$

Substituting Eq. (18) into the time evolution operator in Eq. (13) enables us to give out the time evolution operator in Floquet representation.[50,51]

We now expand the reduced density matrix in a basis of harmonic oscillator eigenstates $(H_0|i\rangle = \varepsilon_0(i)|i\rangle, H_1|i'\rangle = \varepsilon_1(i')|i'\rangle)$,

$$\begin{aligned}\frac{d\rho_0(i,j)}{dt} = &-\frac{i}{\hbar}(\varepsilon_0(i) - \varepsilon_0(j))\rho_0(i,j) \\ &- \frac{\Gamma}{2\hbar}\sum_{i',k} \tilde{f}(\varepsilon_1(i') - \varepsilon_0(k)) F_{i\to i'} F_{k\to i'} \rho_0(k,j) \\ &+ \frac{\Gamma}{2\hbar}\sum_{i',j'} (1 - \tilde{f}^*(\varepsilon_1(j') - \varepsilon_0(j))) F_{i\to i'} F_{j\to j'} \rho_1(i',j') \\ &- \frac{\Gamma}{2\hbar}\sum_{i',k} \rho_0(i,k)\tilde{f}^*(\varepsilon_1(i') - \varepsilon_0(k)) F_{j\to i'} F_{k\to i'} \\ &+ \frac{\Gamma}{2\hbar}\sum_{i',j'} \rho_1(i',j')(1 - \tilde{f}(\varepsilon_1(i') - \varepsilon_0(i))) F_{i\to i'} F_{j\to j'}, \end{aligned} \quad (20)$$

$$\begin{aligned}\frac{d\rho_1(i',j')}{dt} = &-\frac{i}{\hbar}(\varepsilon_1(i') - \varepsilon_1(j'))\rho_1(i',j') \\ &- \frac{\Gamma}{2\hbar}\sum_{i,k'} (1 - \tilde{f}^*(\varepsilon_1(k') - \varepsilon_0(i))) F_{i\to i'} F_{i\to k'} \rho_1(k',j') \\ &+ \frac{\Gamma}{2\hbar}\sum_{i,j} \tilde{f}(\varepsilon_1(j') - \varepsilon_0(j)) F_{i\to i'} F_{j\to j'} \rho_0(i,j) \\ &- \frac{\Gamma}{2\hbar}\sum_{i,k'} \rho_1(i',k')(1 - \tilde{f}(\varepsilon_1(k') - \varepsilon_0(i))) F_{i\to j'} F_{i\to k'} \\ &+ \frac{\Gamma}{2\hbar}\sum_{i,j} \rho_0(i,j)\tilde{f}^*(\varepsilon_1(i') - \varepsilon_0(i)) F_{i\to i'} F_{j\to j'}. \end{aligned} \quad (21)$$

The above-mentioned equations are referred to as our Floquet quantum master equation (FQME). Here, $\varepsilon_0(i) = \hbar\omega(i + \frac{1}{2})$ and $\varepsilon_1(i') = \hbar\omega(i' + \frac{1}{2}) + \bar{E}_d$. $\bar{E}_d$ is the renormalized impurity energy level,

$$\bar{E}_d \equiv E_d - E_r, \quad (22)$$

where $E_r \equiv g^2/\hbar\ \omega$ is the reorganization energy. F is the Frank–Condon factor,

$$F_{i\to i'} = \langle i'|i\rangle = \int dx \phi_{i'}(x + \sqrt{2}\lambda)\phi_i(x), \lambda \equiv g/\hbar\omega, \quad (23)$$

where $\phi_i(x)$ is the ith eigenfunction of the harmonic oscillator. The Frank–Condon factor can be expressed as

$$F_{i\to i'} = (p!/Q!)^{1/2}\lambda^{Q-p}e^{-\lambda^2/2}L_p^{Q-p}(\lambda^2)[\mathrm{sgn}\,(i'-i)]^{i-i'}. \quad (24)$$

p(Q) is the minimum (maximum) of i and i', and L_n^m is a generalized Laguerre polynomial. $\tilde{f}(x)$ in the above-mentioned equations is the modified Fermi function with Floquet replicas, which is given by

$$\tilde{f}(x) = \sum_{n,m}(i)^n(-i)^m J_n(z)J_m(z)e^{i(n-m)\Omega t}f(x-m\Omega). \quad (25)$$

Notice that $\tilde{f}(x)$ is a time-dependent complex number ($\tilde{f}(x)^*$ is its complex conjugate). When taking time average over a cycle, we arrive at the time-independent modified Fermi function,

$$\bar{f}(x) = \sum_n J_n(z)^2 f(x-n\Omega). \quad (26)$$

Finally, Γ in Eqs. (20) and (21) is the hybridization function,

$$\Gamma(\varepsilon) = 2\pi\sum_k |V_k|^2\delta(\varepsilon_k-\varepsilon). \quad (27)$$

In the wide band limit, we assume that Γ is a constant (i.e., does not change with ε or x).

C. Floquet classical master equation

In the limit of $kT > \hbar\omega$, we can treat the nuclear motion classically such that we will arrive at the Floquet classical master equation (FCME). The FCME is obtained by taking the Wigner transform of the FQME [Eqs. (20) and (21)], similar to the steps taken in Ref. 46,

$$\frac{\partial P_0(x,p)}{\partial t} = \frac{\partial H_0(x,p)}{\partial x}\frac{\partial P_0(x,p)}{\partial p} - \frac{\partial H_0(x,p)}{\partial p}\frac{\partial P_0(x,p)}{\partial x} - \gamma_{0\to1}P_0(x,p) + \gamma_{1\to0}P_1(x,p), \quad (28)$$

$$\frac{\partial P_1(x,p)}{\partial t} = \frac{\partial H_1(x,p)}{\partial x}\frac{\partial P_1(x,p)}{\partial p} - \frac{\partial H_1(x,p)}{\partial p}\frac{\partial P_1(x,p)}{\partial x} + \gamma_{0\to1}P_0(x,p) - \gamma_{1\to0}P_1(x,p), \quad (29)$$

where

$$\gamma_{0\to1}(t) = \frac{\Gamma}{\hbar}\Re(\tilde{f}(\Delta V)), \quad (30)$$

$$\gamma_{1\to0}(t) = \frac{\Gamma}{\hbar}(1-\Re(\tilde{f}(\Delta V))), \quad (31)$$

$$\Delta V = H_1 - H_0 = E_d + \sqrt{\frac{2M\omega}{\hbar}}gx. \quad (32)$$

$\tilde{f}(\Delta V)$ is given in Eq. (25). Note that only the real part of $\tilde{f}(\Delta V)$ is used for the hopping rate. As we can see from the above-mentioned equations, the hopping rates here are time-dependent. When using $\bar{f}(\Delta V)$ in Eq. (26), we can get the time-independent hopping rates $\bar{\gamma}_{0\to1}$ and $\bar{\gamma}_{1\to0}$.

The Floquet CME is similar to the non-Floquet CME,[46] except that the Fermi function is modified with Floquet replicas. In the non-Floquet CME, $\gamma_{0\to1}$ ($\gamma_{1\to0}$) is a real positive number and can be interpreted as the hopping rates such that the detailed balance is achieved. In the Floquet CME, however, the modified $\gamma_{0\to1}$ ($\gamma_{1\to0}$) can be negative. Such negative valued rates will not result in hopping events in our surface hopping (see our algorithm below). Still, in the limit of fast driving (large Ω), we can take the time average of the modified Fermi function such that $\bar{\gamma}_{0\to1}$ ($\bar{\gamma}_{1\to0}$) will become real positive valued. Below, we will use a trajectories based surface hopping algorithm to solve the Floquet CME.

D. Floquet surface hopping

As stated above, the Floquet CME is similar to the non-Floquet CME in form, except the hopping rates have negative values. We now introduce three surface hopping algorithms to solve the Floquet CME:

(1) FSH: in FSH, we interpret the real positive part of $\gamma_{0\to1}$ as our hopping rates and determine a hopping event from state $|0\rangle$ to state $|1\rangle$ based on $\xi < \gamma_{0\to1}dt$, where ξ is a random number between 0 and 1, such that the negative valued hopping rates will be automatically discarded. Similarly, a hopping event from state $|1\rangle$ to state $|0\rangle$ is determined by $\xi < \gamma_{1\to0}dt$.
(2) FaSH: in FaSH, we take the time average of $\tilde{f}(\Delta V)$ over a cycle that becomes $\bar{f}(\Delta V)$ such that the hopping rates are real valued and determine the hopping probability.
(3) FaSH-density: in FaSH-density, we use the time-averaged $\bar{f}(\Delta V)$ as our hopping rates to propagate nuclear dynamics as same as FasH. In addition, we propagate electron density using $\dot{P}_0 = -\gamma_{0\to1}P_0 + \gamma_{1\to0}P_1$ and $\dot{P}_1 = \gamma_{0\to1}P_0(x,p) - \gamma_{1\to0}P_1(x,p)$. Here, $\gamma_{0\to1}$ and $\gamma_{1\to0}$ are non-time-averaged such that we can capture the oscillation in a cycle for electronic dynamics.

We initialize our nuclei in one well (the unoccupied electronic state) with a Boltzmann distribution. Notice that the initial nuclei temperature can be different from the electronic temperature such that we can simulate the energy relaxation of the nuclear kinetic energy. In the realistic calculation, we need to truncate for the hopping rates. The Bessel function $J_n(z)$ appearing in Eqs. (25) and (26) decreases with the increase in n when fixing z; thus, we can choose the largest n to confirm $J_n(z) \to 0$. For different $z = \frac{A}{\Omega}$, we need to choose a different number n to make sure the convergence of the hopping rates. For Floquet surface hopping, we average the results over 10 000 trajectories.

III. RESULTS

We now benchmark our trajectory based algorithms against FQME for electronic population as well as nuclear kinetic energy.

We first look at the electronic population with periodic driving as a function of time. In Fig. 1(a), we show the electronic population dynamics from FQME and FSH at different temperatures ($kT = 0.25, 0.5, 1$). Here, we set the nuclear vibration frequency as $\hbar\omega = 0.3$. As expected, at high temperatures ($kT > \hbar\omega$), FSH agrees with the FQME very well, whereas at low temperatures, FSH shows discrepancies as compared to FQME. A similar trend is observed for

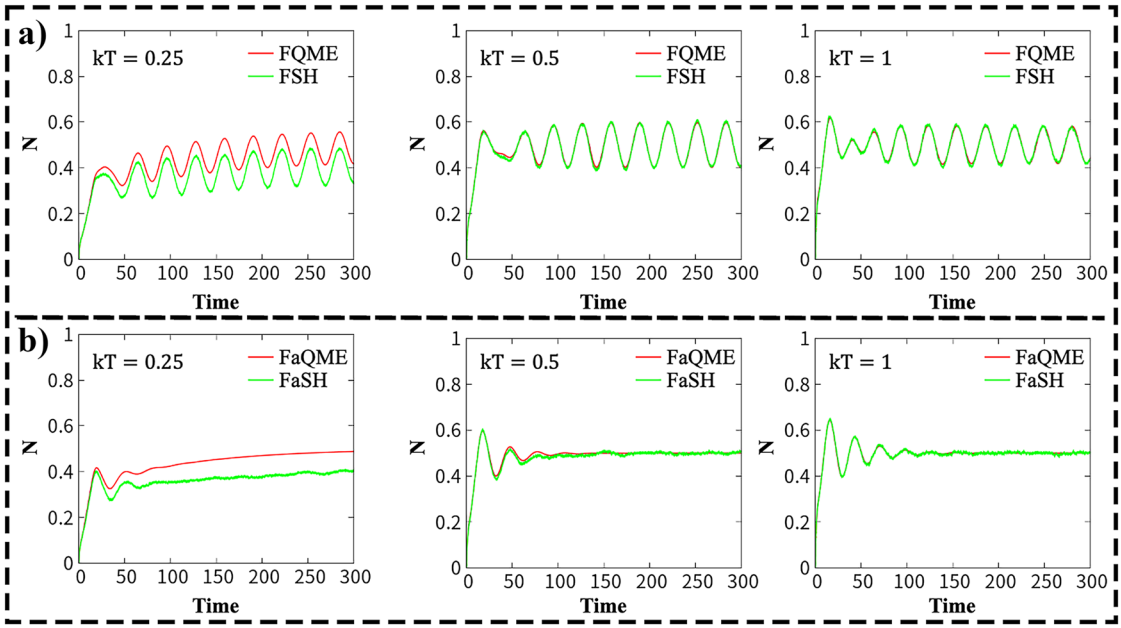

FIG. 1. The impurity electronic population as a function of time for (a) non-time-averaged FQME and FSH; (b) time-averaged FaQME and FaSH. $\Gamma = 1, \hbar\omega = 0.3$, el–ph coupling $g = 0.75$, and $\bar{E}_d = 0$. The driving amplitude is $A = 0.2$, and the driving frequency is $\Omega = 0.2$. Note that FSH and FaSH agree with the FQME and FaQME at high temperatures. At time zero, the phonon is prepared to be equilibrated thermally at an unoccupied impurity level.

FaSH and FaQME as shown in Fig. 1(b): in the high temperature limit, FaSH agrees with the FaQME very well. Notice that the time-averaged Floquet results (FaSH or FaQME) do not show oscillations and reach a steady state in the long time. The non-time-averaged methods (FSH or FQME) do show the oscillations due to the non-vanishing driving. In the long time, FSH or FQME reaches a cycle limit instead of a steady state. The frequency of the oscillation in the electronic population is equal to the frequency of the driving (we have set $\Omega = 0.2$).

To further verify our methods, we show the electronic population and phonon relaxation dynamics as a function of time without any Floquet driving in Fig. 2. In such a case, we expect that the five algorithms (FQME, FSH, FaQME, FaSH, and FaSH-density) should all agree with each other at high temperatures. Indeed, for the case of $kT > \hbar\omega$ ($kT = 1$ and $\hbar\omega = 0.3$), the algorithms all agree with each other for both electronic population [Fig. 2(a)] and nuclear kinetic energy [Fig. 2(b)]. Obviously, without any Floquet driving, both electronic population and nuclear kinetic energy reach a steady state or an equilibrium state. Indeed, the steady-state kinetic energy is $E_k = 1/2kT$ and the electronic population is $N = f(\bar{E}_d)$. Here, kT is the temperature of the electronic bath. Below, we will mainly look at the high temperature limit where the classical nuclei are valid.

In Fig. 3, we benchmark our algorithms for relatively small driving amplitudes with different driving frequencies. Here, the driving amplitude is $A = 0.2$, which is comparable to the nuclear frequency ($\hbar\omega = 0.3$). In such a case, all five methods agree with each other regardless of the driving frequencies. That being said, the non-time-averaged methods (FSH, FQME, and FaSH-density) do show small oscillations in electronic dynamics. The steady states of electronic population and nuclear kinetics in this case are very close to the equilibrium states with $E_k = 1/2kT$ and $N = f(\bar{E}_d)$.

We now turn to the intermediate driving amplitude, where we have set $A = 1$. In such a case, the five methods start to

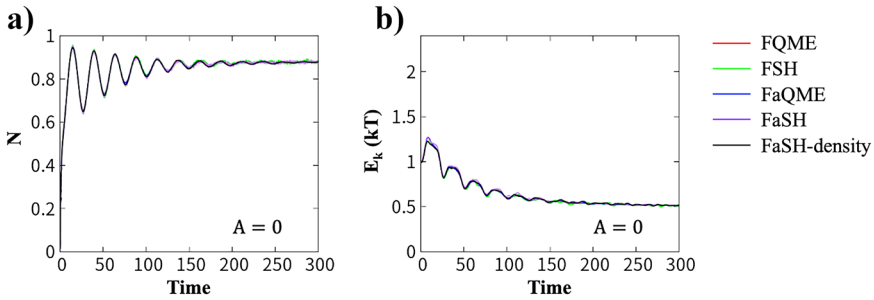

FIG. 2. We show (a) the impurity electronic population and (b) the phonon relaxation as a function of time without Floquet engineering for the five methods, i.e., FQME, FSH, FaQME, FaSH, and FaSH-density. $kT = 1$, $\Gamma = 1$, $\hbar\omega = 0.3$, el–ph coupling $g = 0.75$, and $\bar{E}_d = -2$. Note that without Floquet engineering, the five approaches show exactly the same results.

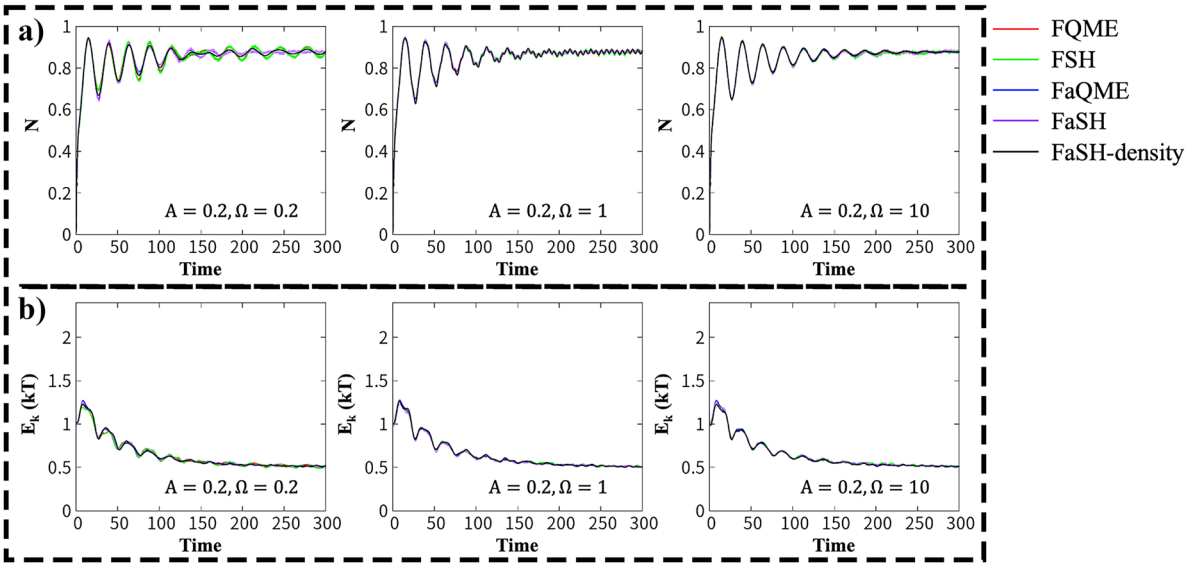

FIG. 3. (a) The impurity electronic population as a function of time under a small strength of driving amplitude that is comparable with the nuclear oscillator ($A = 0.2$) with three degrees of driving frequencies ($\Omega = 0.2, 1,$ and 10). $kT = 1$, $\Gamma = 1$, $\hbar\omega = 0.3$, el–ph coupling $g = 0.75$, and $\bar{E}_d = -2$. The five methods, i.e., FQME, FSH, FaQME, FaSH, and FaSH-density, are put together for comparison. Note that at small strength of the drivings, the five methods give nearly the same feature of electronic and nuclear dynamics as that in Fig. 2, regardless of the driving frequencies.

show deviations, as shown in Fig. 4. For smaller driving frequencies (e.g., $\Omega = 0.5$), the oscillation feature from the FQME and FSH becomes stronger in both electronic population and nuclear dynamics, whereas FaSH and FaQME miss the feature completely. FaSH-density shows oscillation in electronic dynamics and fails to reproduce the feature in nuclear dynamics. For a slightly larger driving frequency ($\Omega = 1$ or 10), the oscillation feature becomes weaker. However, FSH starts to show deviations in the steady state at a very

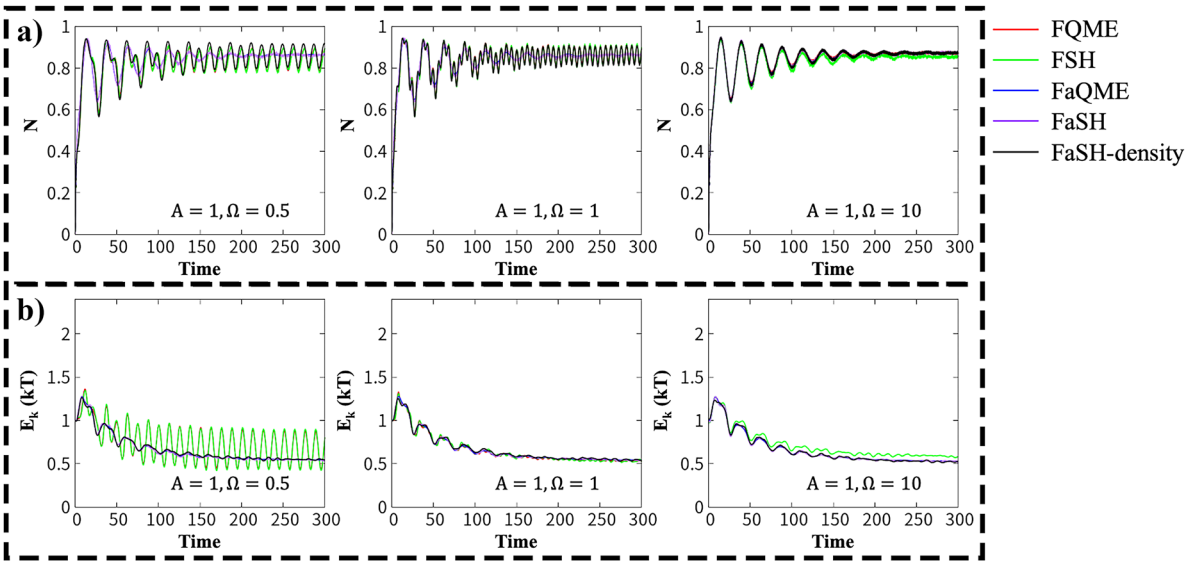

FIG. 4. (a) The impurity electronic population as a function of time under a medium strong driving amplitude ($A = 1$) with three degrees of driving frequencies ($\Omega = 0.5, 1,$ and 10). $kT = 1$, $\Gamma = 1$, $\hbar\omega = 0.3$, el–ph coupling $g = 0.75$, and $\bar{E}_d = -2$. We compare the five methods, i.e., FQME, FSH, FaQME, FaSH, and FaSH-density, for intermediate driving amplitudes. Note that the time-averaged FaQME and FaSH cannot capture the oscillation feature in both electronic and nuclear dynamics, especially under slow and medium quick drivings ($\Omega = 0.5$ or $\Omega = 1$). FSH does not obey the detailed balance, resulting in a higher effective temperature at a large driving frequency ($\Omega = 10$). The FaSH-density method enables us to capture the oscillation feature in electronic dynamics and results in the correct effective temperature at large Ω.

large driving frequency ($\Omega = 10$), where the kinetic energy is higher than the results from FQME (and others). Consequently, the electronic population from FSH is smaller than the results from other methods. This deviation under quick drivings is mainly derived from disregarding the negative part of the hopping rate in the FSH algorithm, which violates the detailed balance. As a result, the effective temperature of the system from FSH is higher than the true effective temperature from other methods. Note also that the true effective temperature is slightly different from the equilibrium temperature. This is due to the effects of the driving.

Finally, we show the case of a very strong driving amplitude ($A = 4$) in Fig. 5. In such a case, the oscillation feature becomes very strong, particularly for small driving amplitudes. Again, FSH works very well at small driving frequencies but fails to produce the steady states of electronic population and nuclear kinetic energy at large driving frequencies. FaSH misses all oscillation features at small driving frequencies but does reach correct steady states. FaSH-density performs the best, working at both small driving frequencies and large driving frequencies.

Overall, we propose three Floquet surface hopping algorithms that are appropriate in the high temperature limit ($kT > \hbar\omega$). The FaSH method works well in fast drivings ($\frac{A}{\hbar\Omega}$ is small), while fails in slow drivings ($\frac{A}{\hbar\Omega}$ is large) due to the time average. The FSH method works well in slow drivings, while it fails in fast drivings due to its negative hopping rates. The FaSH-density method is appropriate for all kinds of drivings.

IV. CONCLUSIONS

In summary, we derived the Floquet quantum master equation to study the dynamics of a periodically driven system near a metal surface. At the high temperature limit, the FQME reduces to a FCME. We proposed three surface hopping algorithms (FSH, FaSH, and FaSH-density) to solve the FCME. In the limit of small driving frequencies, FSH works very well, capturing the full dynamics for both electronic population and nuclear kinetic energy as being benchmarked against FQME. At large driving frequencies, FSH fails to produce the correct steady states. This is due to the fact that we throw out the negative hopping rates in FSH. The FaSH works well at large driving frequencies but fails to reproduce the oscillation features at small driving frequencies. The FaSH-density performs the best, which reproduces the full electronic dynamics at small and large driving frequencies and reaches the correct steady states for nuclear motion. In the future, we will go beyond the one level case and study the multiple-level case in the molecule near metal surfaces and under periodic driving such that we will need to embed a Floquet quantum–classical Liouville equation (FQCLE) into a CME. Such work is under investigation.[47]

ACKNOWLEDGMENTS

We thank Amikam Levy, Jacob Bätge, and Michael Thoss for useful and inspiring conversations. This material is based upon work

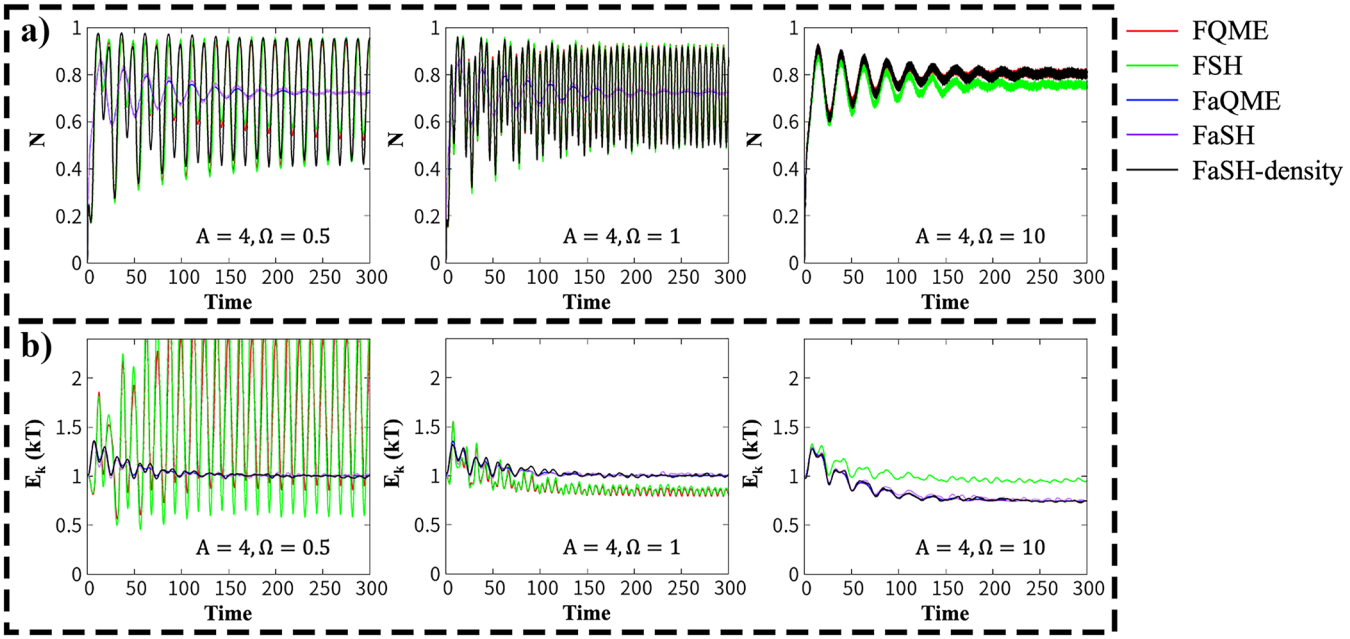

FIG. 5. (a) The impurity electronic population as a function of time under a strong driving amplitude ($A = 4$) for small and large driving frequencies ($\Omega = 0.5, 1,$ and 10). $kT = 1$, $\Gamma = 1$, $\hbar\omega = 0.3$, el–ph coupling $g = 0.75$, and $\bar{E}_d = -2$. Again, the time-averaged FaQME and FaSH cannot capture the oscillation feature under slow and medium quick drives ($\Omega = 0.5$ or $\Omega = 1$). FSH gives rise to wrong steady-state results under a quick drive ($\Omega = 10$). FaSH-density performs the best, which enables us to capture the oscillation feature for electronic dynamics and gives rise to proper steady-state results.

supported by the National Natural Science Foundation of China (NSFC Grant No. 22273075).

AUTHOR DECLARATIONS

Conflict of Interest

The authors have no conflicts to disclose.

Author Contributions

Yu Wang: Writing – original draft (equal). **Wenjie Dou**: Methodology (equal).

DATA AVAILABILITY

The data that support the findings of this study are available from the corresponding author upon reasonable request.

REFERENCES

[1]T. Oka and S. Kitamura, "Floquet engineering of quantum materials," Annu. Rev. Condens. Matter Phys. **10**, 387–408 (2019).
[2]M. Hertzog, M. Wang, J. Mony, and K. Börjesson, "Strong light–matter interactions: A new direction within chemistry," Chem. Soc. Rev. **48**, 937–961 (2019).
[3]F. J. Garcia-Vidal, C. Ciuti, and T. W. Ebbesen, "Manipulating matter by strong coupling to vacuum fields," Science **373**, eabd0336 (2021).
[4]E. Orgiu, J. George, J. A. Hutchison, E. Devaux, J. F. Dayen, B. Doudin, F. Stellacci, C. Genet, J. Schachenmayer, C. Genes *et al.*, "Conductivity in organic semiconductors hybridized with the vacuum field," Nat. Mater. **14**, 1123–1129 (2015).
[5]K. Nagarajan, J. George, A. Thomas, E. Devaux, T. Chervy, S. Azzini, K. Joseph, A. Jouaiti, M. W. Hosseini, A. Kumar *et al.*, "Conductivity and photoconductivity of a p-type organic semiconductor under ultrastrong coupling," ACS Nano **14**, 10219–10225 (2020).
[6]C. Gonzalez-Ballestero, J. Feist, E. Moreno, and F. J. Garcia-Vidal, "Harvesting excitons through plasmonic strong coupling," Phys. Rev. B **92**, 121402 (2015).
[7]S. Hou, M. Khatoniar, K. Ding, Y. Qu, A. Napolov, V. M. Menon, and S. R. Forrest, "Ultralong-range energy transport in a disordered organic semiconductor at room temperature via coherent exciton-polariton propagation," Adv. Mater. **32**, 2002127 (2020).
[8]X. Zhong, T. Chervy, L. Zhang, A. Thomas, J. George, C. Genet, J. A. Hutchison, and T. W. Ebbesen, "Energy transfer between spatially separated entangled molecules," Angew. Chem., Int. Ed. **56**, 9034–9038 (2017).
[9]D. G. Lidzey, A. M. Fox, M. D. Rahn, M. S. Skolnick, V. M. Agranovich, and S. Walker, "Experimental study of light emission from strongly coupled organic semiconductor microcavities following nonresonant laser excitation," Phys. Rev. B **65**, 195312 (2002).
[10]D. M. Coles, P. Michetti, C. Clark, W. C. Tsoi, A. M. Adawi, J.-S. Kim, and D. G. Lidzey, "Vibrationally assisted polariton-relaxation processes in strongly coupled organic-semiconductor microcavities," Adv. Funct. Mater. **21**, 3691–3696 (2011).
[11]D. M. Coles, R. T. Grant, D. G. Lidzey, C. Clark, and P. G. Lagoudakis, "Imaging the polariton relaxation bottleneck in strongly coupled organic semiconductor microcavities," Phys. Rev. B **88**, 121303 (2013).
[12]S. Wang, T. Chervy, J. George, J. A. Hutchison, C. Genet, and T. W. Ebbesen, "Quantum yield of polariton emission from hybrid light-matter states," J. Phys. Chem. Lett. **5**, 1433–1439 (2014).
[13]D. Ballarini, M. De Giorgi, S. Gambino, G. Lerario, M. Mazzeo, A. Genco, G. Accorsi, C. Giansante, S. Colella, S. D'Agostino *et al.*, "Polariton-induced enhanced emission from an organic dye under the strong coupling regime," Adv. Opt. Mater. **2**, 1076–1081 (2014).
[14]R. T. Grant, P. Michetti, A. J. Musser, P. Gregoire, T. Virgili, E. Vella, M. Cavazzini, K. Georgiou, F. Galeotti, C. Clark *et al.*, "Efficient radiative pumping of polaritons in a strongly coupled microcavity by a fluorescent molecular dye," Adv. Opt. Mater. **4**, 1615–1623 (2016).
[15]K. Stranius, M. Hertzog, and K. Börjesson, "Selective manipulation of electronically excited states through strong light–matter interactions," Nat. Commun. **9**, 2273 (2018).
[16]J. A. Hutchison, T. Schwartz, C. Genet, E. Devaux, and T. W. Ebbesen, "Modifying chemical landscapes by coupling to vacuum fields," Angew. Chem., Int. Ed. **51**, 1592–1596 (2012).
[17]L. Lin, M. Wang, X. Wei, X. Peng, C. Xie, and Y. Zheng, "Photoswitchable rabi splitting in hybrid plasmon–waveguide modes," Nano Lett. **16**, 7655–7663 (2016).
[18]J. Feist, J. Galego, and F. J. Garcia-Vidal, "Polaritonic chemistry with organic molecules," ACS Photonics **5**, 205–216 (2018).
[19]X. Li, A. Mandal, and P. Huo, "Cavity frequency-dependent theory for vibrational polariton chemistry," Nat. Commun. **12**, 1315 (2021).
[20]H. Hübener, U. De Giovannini, C. Schäfer, J. Andberger, M. Ruggenthaler, J. Faist, and A. Rubio, "Engineering quantum materials with chiral optical cavities," Nat. Mater. **20**, 438–442 (2021).
[21]M. Thoss, I. Kondov, and H. Wang, "Correlated electron-nuclear dynamics in ultrafast photoinduced electron-transfer reactions at dye-semiconductor interfaces," Phys. Rev. B **76**, 153313 (2007).
[22]L. Mühlbacher and E. Rabani, "Real-time path integral approach to nonequilibrium many-body quantum systems," Phys. Rev. Lett. **100**, 176403 (2008).
[23]A. C. Hewson and D. Meyer, "Numerical renormalization group study of the anderson-holstein impurity model," J. Phys.: Condens. Matter **14**, 427–445 (2001).
[24]G. Cabra, I. Franco, and M. Galperin, "Optical properties of periodically driven open nonequilibrium quantum systems," J. Chem. Phys. **152**, 094101 (2020).
[25]K. G. Wilson, "The renormalization group: Critical phenomena and the Kondo problem," Rev. Mod. Phys. **47**, 773–840 (1975).
[26]C. Schinabeck, A. Erpenbeck, R. Härtle, and M. Thoss, "Hierarchical quantum master equation approach to electronic-vibrational coupling in nonequilibrium transport through nanosystems," Phys. Rev. B **94**, 201407 (2016).
[27]J. Jin, X. Zheng, and Y. Yan, "Exact dynamics of dissipative electronic systems and quantum transport: Hierarchical equations of motion approach," J. Chem. Phys. **128**, 234703 (2008).
[28]M. Galperin, M. A. Ratner, and A. Nitzan, "Molecular transport junctions: Vibrational effects," J. Phys.: Condens. Matter **19**, 103201 (2007).
[29]J. R. Reimers, G. C. Solomon, A. Gagliardi, A. Bilić, N. S. Hush, T. Frauenheim, A. Di Carlo, and A. Pecchia, "The green's function density functional tight-binding (gDFTB) method for molecular electronic conduction," J. Phys. Chem. A **111**, 5692–5702 (2007).
[30]N. Bode, S. V. Kusminskiy, R. Egger, and F. von Oppen, "Current-induced forces in mesoscopic systems: A scattering-matrix approach," Beilstein J. Nanotechnol. **3**, 144–162 (2012).
[31]A. V. Akimov and O. V. Prezhdo, "The PYXAID program for non-adiabatic molecular dynamics in condensed matter systems," J. Chem. Theory Comput. **9**, 4959–4972 (2013).
[32]T. Fiedlschuster, J. Handt, and R. Schmidt, "Floquet surface hopping: Laser-driven dissociation and ionization dynamics of H^{2+}," Phys. Rev. A **93**, 053409 (2016).
[33]Z. Zhou, H.-T. Chen, A. Nitzan, and J. E. Subotnik, "Nonadiabatic dynamics in a laser field: Using Floquet fewest switches surface hopping to calculate electronic populations for slow nuclear velocities," J. Chem. Theory Comput. **16**, 821–834 (2020).
[34]H.-T. Chen, Z. Zhou, and J. E. Subotnik, "On the proper derivation of the Floquet-based quantum classical Liouville equation and surface hopping describing a molecule or material subject to an external field," J. Chem. Phys. **153**, 044116 (2020).
[35]M. Schirò, F. G. Eich, and F. Agostini, "Quantum–classical nonadiabatic dynamics of Floquet driven systems," J. Chem. Phys. **154**, 114101 (2021).
[36]B. H. Wu and J. C. Cao, "Time-dependent multimode transport through quantum wires with spin-orbit interaction: Floquet scattering matrix approach," Phys. Rev. B **73**, 245412 (2006).

[37]M. Moskalets, "Floquet scattering matrix theory of heat fluctuations in dynamical quantum conductors," Phys. Rev. Lett. **112**, 206801 (2014).
[38]P. A. Pantazopoulos and N. Stefanou, "Layered optomagnonic structures: Time Floquet scattering-matrix approach," Phys. Rev. B **99**, 144415 (2019).
[39]F. Capolino, M. Albani, S. Maci, and L. B. Felsen, "Frequency-domain Green's function for a planar periodic semi-infinite phased array. I. Truncated Floquet wave formulation," IEEE Trans. Antennas Propag. **48**, 67–74 (2000).
[40]L. E. F. Foa Torres, "Mono-parametric quantum charge pumping: Interplay between spatial interference and photon-assisted tunneling," Phys. Rev. B **72**, 245339 (2005).
[41]B. Wu and J. Cao, "Noise of Kondo dot with ac gate: Floquet–Green's function and noncrossing approximation approach," Phys. Rev. B **81**, 085327 (2010).
[42]T. D. Honeychurch and D. S. Kosov, "Quantum transport in driven systems with vibrations: Floquet nonequilibrium Green's functions and the self-consistent Born approximation," Phys. Rev. B **107**, 035410 (2023).
[43]S. Kohler, T. Dittrich, and P. Hänggi, "Floquet-Markovian description of the parametrically driven, dissipative harmonic quantum oscillator," Phys. Rev. E **55**, 300 (1997).
[44]B. Wu and C. Timm, "Noise spectra of ac-driven quantum dots: Floquet master-equation approach," Phys. Rev. B **81**, 075309 (2010).
[45]M. Kuperman, L. Nagar, and U. Peskin, "Mechanical stabilization of nanoscale conductors by plasmon oscillations," Nano Lett. **20**, 5531–5537 (2020).
[46]W. Dou, A. Nitzan, and J. E. Subotnik, "Surface hopping with a manifold of electronic states. III. Transients, broadening, and the Marcus picture," J. Chem. Phys. **142**, 234106 (2015).
[47]V. Mosallanejad, Y. Wang, J. Chen, and W. Dou, "Floquet nonadiabatic dynamics in open quantum systems," arXiv:2303.08501 (2023).
[48]M. Hartmann, D. Poletti, M. Ivanchenko, S. Denisov, and P. Hänggi, "Asymptotic Floquet states of open quantum systems: The role of interaction," New J. Phys. **19**, 083011 (2017).
[49]T. Mori, "Floquet states in open quantum systems," Annu. Rev. Condens. Matter Phys. **14**, 35–56 (2023).
[50]J. H. Shirley, "Solution of the Schrödinger equation with a Hamiltonian periodic in time," Phys. Rev. **138**, B979 (1965).
[51]K. L. Ivanov, K. R. Mote, M. Ernst, A. Equbal, and P. K. Madhu, "Floquet theory in magnetic resonance: Formalism and applications," Prog. Nucl. Magn. Reson. Spectrosc. **126–127**, 17–58 (2021).